Phenotypic variability in chloroplast redox state predicts cell fate in a marine diatom

Avia Mizrachi[a], Shiri Graff van Creveld[a], Orr H. Shapiro[b], Shilo Rosenwasser[a,c], and Assaf Vardi[a,1].

[a]Department of Plant and Environmental Sciences, Weizmann Institute of Science, 7610001 Rehovot, Israel.
[b]Department of Food Quality and Safety, Institute for Postharvest and Food Sciences, Agricultural Research Organization, The Volcani Center, Rishon LeZion 7528809, Israel.
[c]The Robert H. Smith Institute of Plant Sciences and Genetics in Agriculture, The Hebrew University of Jerusalem, 7610001 Rehovot, Israel.
[1]To whom correspondence should be addressed. Email: assaf.vardi@weizmann.ac.il

Short title: Chloroplast redox variability predicts cell fate

Abstract

Diatoms are photosynthetic microorganisms of great ecological and biogeochemical importance, forming vast blooms in diverse aquatic ecosystems. They are subjected to a wide range of environmental cues, including abiotic stressors and biotic interactions with associated bacteria, viruses and grazers. However, the cellular strategies that underline their ecological success and their rapid acclimation to fluctuating conditions are still underexplored. This study investigates heterogeneity within diatom populations in response to oxidative stress, which mediates a wide range of environmental stress conditions. We combined flow cytometry and microfluidics system for live-imaging microscopy to measure redox dynamics at the single-cell level. Using the redox-sensitive sensor roGFP we measured *in vivo* organelle-specific oxidation patterns in the model diatom *Phaeodactylum tricornutum*. Chloroplast targeted roGFP exhibited a light-dependent, bi-stable oxidation pattern in response to oxidative stress, revealing two distinct subpopulations. Remarkably, the "oxidized" subpopulation was sensitive to the stress and subsequently died, while the "reduced" subpopulation was resilient to it and recovered. We further characterized an early phase of "pre-commitment" to cell death following oxidative stress, after which cell death was irreversibly activated in the "oxidized" cells, even upon removal of the stress. Oxidation of the chloroplast glutathione pool preceded commitment to cell death, and was used as a novel predictor of cell fate. We propose that phenotypic variability within diatom populations can provide an ecological strategy to cope with rapid environmental fluctuations in the marine ecosystem.

Significance

Diatoms are responsible for ~20% of photosynthesis on Earth, and are central to biogeochemical cycles. They are constantly exposed to fluctuating conditions of light, nutrients and chemical cues. Until now, our understanding of acclimation strategies in phytoplankton has been based primarily on analysis at the population level. Here we investigate phenotypic variability in the redox response of diatoms to oxidative stress, which mediates diverse environmental stress conditions. Using single-cell approaches, we revealed two distinct subpopulations differing in their chloroplast redox response and subsequent cell fate. These approaches are used as a novel platform to study intraspecies heterogeneity, and shed light on stress sensing

and cell fate regulation. Individuality in stress response may provide a “bet-hedging” strategy beneficial in fluctuating environments.

Introduction

Diatoms are considered to be amongst the most successful and diverse eukaryotic phytoplankton groups, and are estimated to contribute 20% of global net primary production (1–3). They form massive blooms and are thus central to the biogeochemical cycling of important elements such as carbon, nitrogen, phosphate, iron and silica, in addition to their important role at the base of marine food webs (1, 2, 4–6). As other phytoplankton, diatoms need to constantly acclimate to physicochemical gradients in a fluctuating environment. They are exposed to stress from different biotic and abiotic origins such as grazing, viral and bacterial infections, allelopathic interactions, light availability, and nutrient limitations (7–14). Importantly, induction of programmed cell death (PCD) in response to different stressors has been suggested as a major mechanism contributing to the fast turnover of phytoplankton and the rapid demise of their blooms (7, 8, 15).

Recent studies suggested that diatoms possess a signaling mechanism based on compartmentalized redox in response to various environmental cues (16–18). Reactive oxygen species (ROS) are known to play an important role in sensing stress and external signals across kingdoms, from bacteria to plants and animals (19–23). They are produced as byproducts of oxygen-based metabolism in respiration and photosynthesis, by ROS generating enzymes, and due to various stress conditions that lead to their accumulation (16, 22, 24–27). To maintain redox balance and avoid oxidative damage, cells harbor various ROS scavenging enzymes and small antioxidant molecules that regulate and buffer ROS levels, such as glutathione (GSH), ascorbate and NADPH. ROS can cause fast post-translational modifications of proteins through oxidation, affecting their activity even prior to changes in gene expression (22). The specificity of the ROS signal is derived from the specific chemical species, its concentration, sub-cellular localization, temporal dynamics, and available downstream ROS-sensitive targets (16, 22, 24, 28–30). Therefore, ROS production and redox metabolic networks can be used to sense and integrate information of both the metabolic state of the cell and its microenvironment.

H_2O_2 is a relatively mild and stable ROS that can accumulate in cells due to various stress conditions, and thus often serves as a signaling molecule (19–23, 31). It has a preferential activity towards cysteine residues, and it can remodel the redox-sensitive proteome network (17, 23, 28). In addition, it can diffuse across membranes (depending on membrane properties) and through aquaporins channels (32). Combined properties as lower toxicity, diffusibility and selective reactivity make H_2O_2 suitable for studying signaling in various biological systems (23, 28). Since many environmental stressors induce ROS generation, application of H_2O_2 can reproduce the downstream cellular response. H_2O_2 application in marine diatoms led to oxidation patterns similar to other environmental stressors (16, 17). It also led to the induction of cell death, in a dose-dependent manner, with characteristics of PCD that included externalization of phosphatidylserine, DNA laddering, and compromised cell membrane (16–18). In addition, early oxidation of the mitochondrial GSH redox potential (E_{GSH}), which represents the balance between GSH and its oxidized form (GSSG), preceded subsequent cell death at the population level following exposure to H_2O_2 and diatom-derived infochemicals in the diatom *Phaeodactylum tricornutum* (16).

In this work, we investigated phenotypic variability within diatom populations in response to oxidative stress, which may expose a differential response within the population to environmental stressors. We established

single-cell approaches to measure *in vivo* oxidation dynamics in the model diatom *P. tricornutum* using flow cytometry and microfluidics live-imaging. To measure oxidation dynamics of specific organelles, we used *P. tricornutum* strains expressing redox-sensitive GFP (roGFP) targeted to various sub-cellular compartments. The oxidation of roGFP is reversible, and can be quantified using ratiometric fluorescence measurements (33). The roGFP oxidation degree (OxD) represents E_{GSH}, providing a metabolic input of the redox state of the cell and correlates with the oxidation state of native proteins in the organelle (17, 33). By measuring redox dynamics at single-cell resolution, we uncovered a previously uncharacterized phenotypic heterogeneity in the response of marine diatoms to oxidative stress. We revealed a bi-stable response in the chloroplast E_{GSH} following H_2O_2 treatment, exposing distinct subpopulations with different cell fates. Our results revealed a specific link between oxidation patterns in the chloroplast and subsequent cell fate regulation.

Results

Bi-stable chloroplast roGFP oxidation in response to oxidative stress reveals distinct subpopulations.

To assess the roGFP oxidation state in an organelle-specific manner, we measured OxD in *P. tricornutum* strains expressing roGFP targeted to the chloroplast, nucleus and mitochondria using flow cytometry. At steady-state conditions without perturbations, the OxD distribution in the population had a single distinct peak, representing a reduced state at all examined compartments (Fig. 1 A, E, I and Figs. S1, S2). Application of H_2O_2 led to organelle-specific and dose-dependent oxidation patterns in these organelles (Fig. 1).

The chl-roGFP exhibited a distinct bi-stable response following treatments of 50-100µM H_2O_2, revealing two distinct subpopulations of “oxidized” and “reduced” cells (Fig. 1 B-D and Fig. S3 A-C). These subpopulations emerged within the first few minutes post H_2O_2 treatment (Fig. 1 B-D). In the “oxidized” subpopulation, roGFP completely oxidized in response to H_2O_2, reaching a similar distribution of the fully oxidized positive control (200µM H_2O_2) (Fig. 1 B-D and Fig. S3 G). In the “reduced” subpopulation, roGFP reached lower values of 30-43% OxD within 2-24 minutes post treatments, and then gradually recovered (Fig. 1 B-D and Fig. S3 G). Only a minor fraction of the cells displayed intermediate oxidation, suggesting that these subpopulations represent discrete redox states. Interestingly, a larger fraction of cells was within the “oxidized” subpopulation at 20-25 minutes post treatment compared to later time points, indicating that some cells were able to recover during this time (Fig. 1 M). The proportion between these subpopulations stabilized after 46-51 min post treatment, and was H_2O_2-dose dependent, as more cells were within the “oxidized” subpopulation at higher H_2O_2 concentrations (Fig. 1 A-D, M). The emergence of stable co-existing “oxidized” and “reduced” subpopulations revealed underlying heterogeneity within the diatom population, resulting in a differential response to oxidative stress.

This clear bi-stable pattern was unique to the chloroplast E_{GSH}. The nuclear roGFP displayed a continuous distribution in response to H_2O_2 treatments, and no distinct subpopulations could be observed (Fig. 1 F-H). Nuclear roGFP exhibited fast oxidation within a few minutes post treatment, even in response to a low H_2O_2 concentration of 50µM, which had only a mild effect on the chloroplast (Fig. 1 B, F). At that concentration, nuc-roGFP oxidation was followed by a gradual and much slower recovery, which lasted >5 hours post

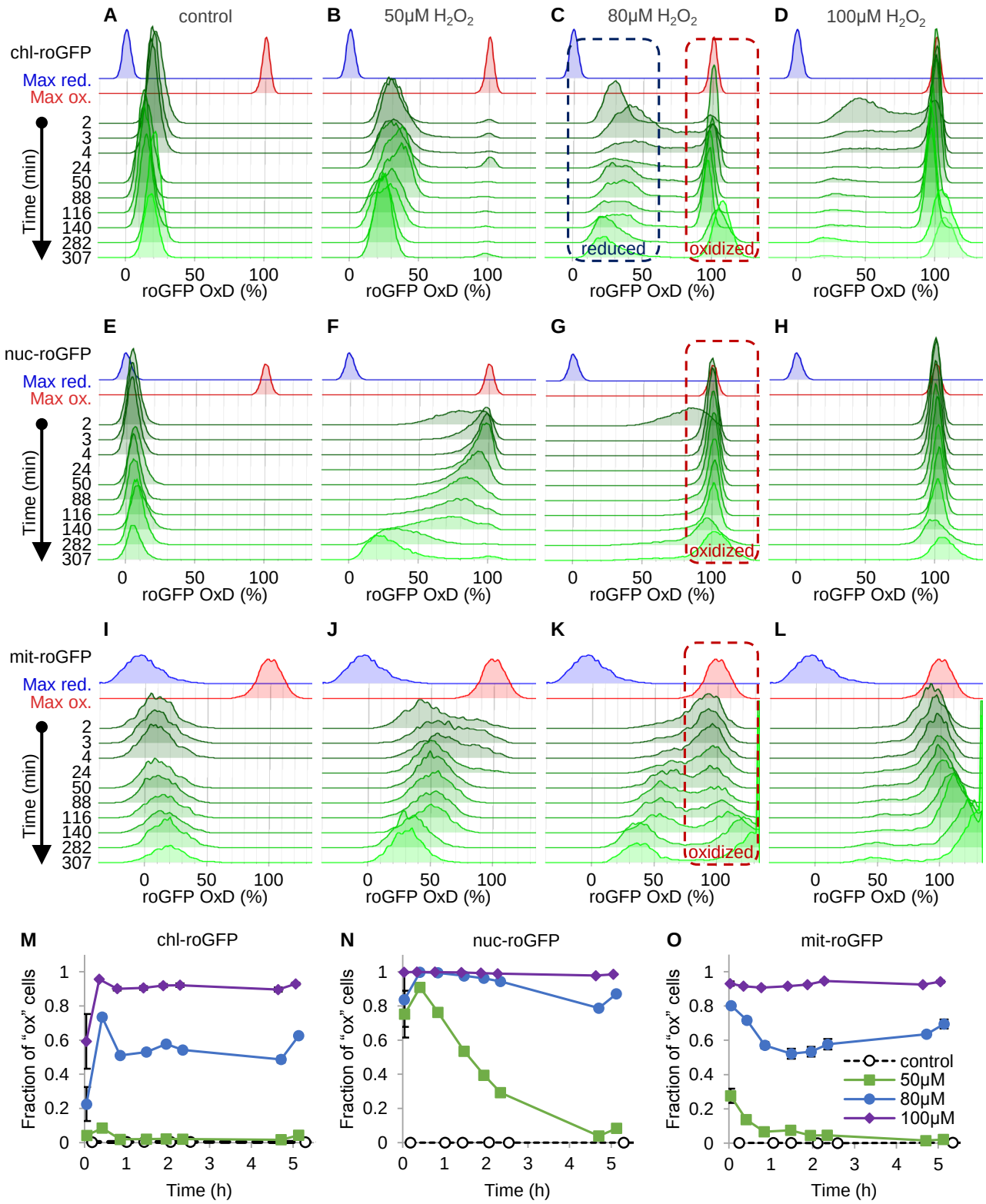

Fig. 1. Oxidation of roGFP in response to H_2O_2 is organelle-specific and reveals heterogeneity at the single-cell level. The distribution of roGFP OxD in the population over time was measured by flow cytometry in *P. tricornutum* cells expressing roGFP targeted to the chloroplast (chl-roGFP, A-D, M), nucleus (nuc-roGFP, E-H, N) and mitochondria (mit-roGFP, I-L, O). (*A-L*) Oxidation of roGFP in response to 0μM (A,E,I), 50μM (B,F,J), 80μM (C,G,K), and 100μM (D,H,L) H_2O_2. Maximum reduction (blue) and oxidation (red) of roGFP following additions of 2mM DTT or 200μM H_2O_2 respectively are shown as reference. The "oxidized" and "reduced" subpopulations are marked by red and blue dashed boxes respectively (C, G, K). The experiment was done in triplicates that were highly similar (data not shown), for visualization the first replica is shown. Each histogram consists of >8000 (A-D), >5900 (E-H) or >1400 (I-L) roGFP-positive cells. (*M-O*) The fraction of

the "oxidized" subpopulation over time upon exposure to 0-100µM H_2O_2. Data is shown as mean ± SEM, n=3. SEM lower than 0.018 is not shown.

treatment (Fig. 1 F). At higher concentrations, the entire population was oxidized within 3 minutes post treatment, and most cells remained stably oxidized >5 hours post treatment (Fig. 1 G-H). The mitochondrial roGFP exhibited a heterogeneous redox response within the diatom population, as seen in the 80µM and 100µM H_2O_2 treatments starting at ~24 minutes post treatment (Fig. 1 K-L). However, distinct subpopulations were not clearly separated until later stages, and were not detected consistently between experiments (Fig. 1 K-L and Fig. S4). Therefore, we chose to focus on the chl-roGFP strain, which revealed two discrete subpopulations.

The bi-stable chloroplast redox response is light dependent.

After observing the distinct chloroplast redox response, we hypothesized that light regime will affect the bi-stable pattern of chl-roGFP following oxidative stress. Photosynthesis is the major source for reductive power as well as ROS in algal cells, and exposure to dark was shown to increase sensitivity to oxidative stress in another marine diatom (18). Therefore, we investigated the effects of short exposure to darkness on the chloroplast redox response. Cells were treated with 0-100µM H_2O_2 and were immediately moved to the dark for 90 minutes, and were then returned to the light ("dark" treated, Fig. 2 and Fig. S5). These cells were compared to cells that were kept in the light during this phase ("light" treated). The transition to the dark caused an immediate oxidation of the basal chl-roGFP OxD (without H_2O_2 treatment), reaching a peak within 15 minutes (Fig. 2 A, D). Then, while still under dark conditions, chl-roGFP showed a gradual reduction without exhibiting a distinct bi-stable distribution of subpopulations (Fig. 2 A, D). Upon shifting back to the light, chl-roGFP reduced within 2 minutes back to its basal state prior to dark exposure (Fig. 2 A, D). The dark mediated oxidation was specific to the chloroplast and was not detected in the nucleus (Fig. S6), demonstrating how signal specificity can be gained by organelle-specific redox perturbations.

The transition to the dark eliminated the bi-stable pattern of chl-roGFP oxidation in response to H_2O_2, and no distinct subpopulations were observed while cells were under darkness (Fig. 2 and Fig. S5). Following treatment of 80µM H_2O_2 and transition to the dark, chl-roGFP fully oxidized in the entire population and remained stably oxidized even after transition back to the light (Fig. 2 C). The bi-stable pattern was regained only upon transition back to the light, and only at lower doses of 30µM and 50µM H_2O_2, in which some or most cells were able to recover following this transition (Fig. 2 B and Fig. S5 C). Therefore, we conclude that the differential redox response of the chloroplast to oxidative stress in the "oxidized" and "reduced" subpopulations was light dependent.

Next, we investigated whether the transition to the dark also affected the diatoms' cell fate. We quantified cell death 24 hours post treatment using flow cytometry measurements of Sytox green staining, which selectively stains nuclei of dead cells. The transition to the dark increased H_2O_2 sensitivity in the entire population, as seen both by the stronger chl-roGFP oxidation and by the larger fraction of dead cells in "dark" compared to "light" treated cells (Fig. 2 and Fig. S5). Taken together, these results demonstrate an important role for chloroplast redox homeostasis and light-dependent reactions in cell fate regulation in diatoms.

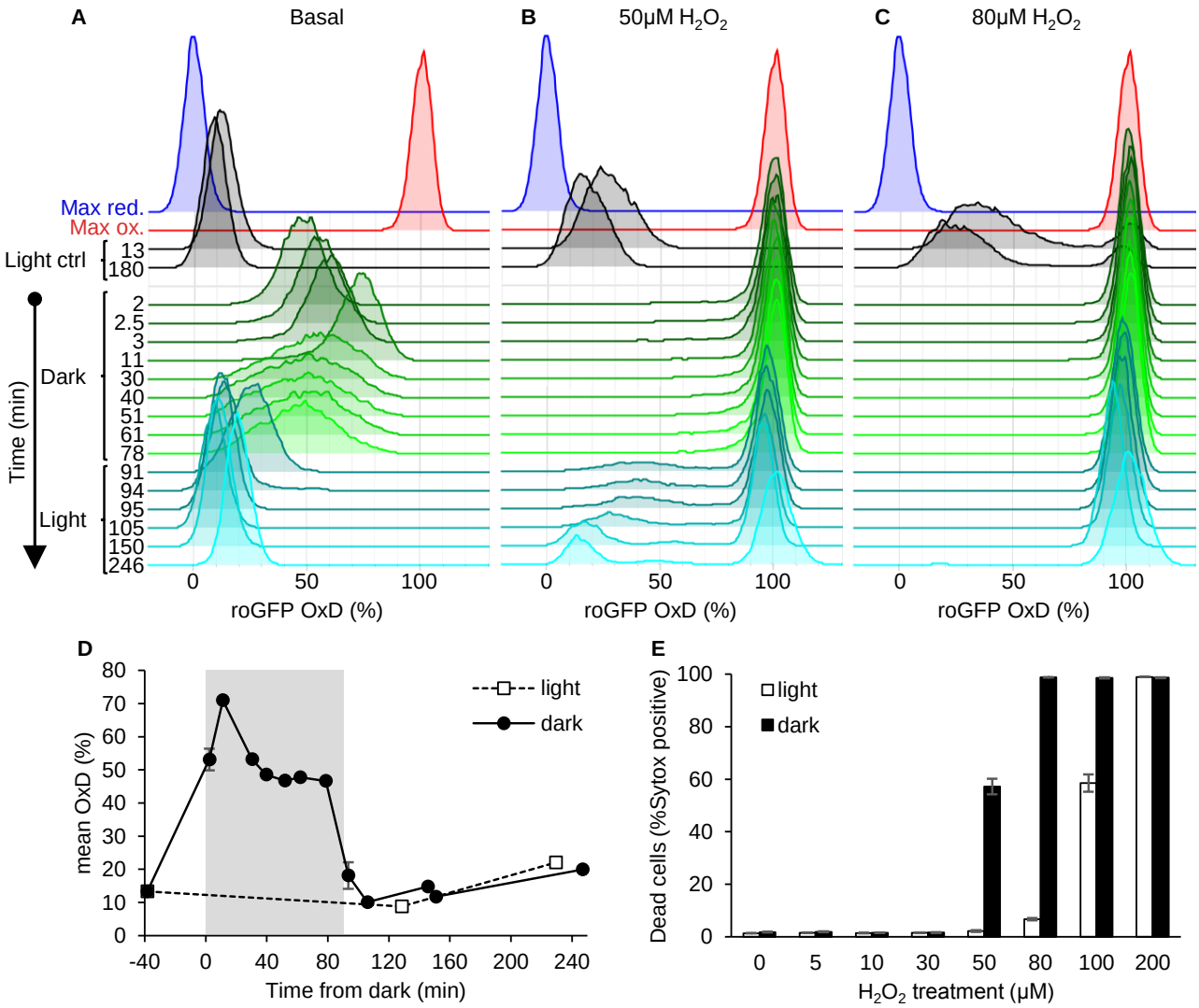

Fig. 2. The bi-stable phenotype in chl-roGFP oxidation in response to H_2O_2 is light-dependent. The effects of a short exposure to darkness on chl-roGFP oxidation patterns were examined. (A-C) Flow cytometry measurements of chl-roGFP OxD distribution in the population over time. Cells were treated with 0µM (control, A), 50µM (B), and 80µM H_2O_2 (C), and were then transitioned to the dark within 5 minutes post treatment (time 0). Cells were kept in the dark for 90 minutes (green) and were then transferred back to the light (cyan). The same H_2O_2 treatment without transition to the dark (black) and maximum oxidation (200µM H_2O_2, red) and reduction (2mM DTT, blue) are shown for reference. The experiment was done in triplicates that were highly similar, for visualization the first replica is shown. Each histogram consists of >8000 cells. (*D*) Mean ± SEM basal chl-roGFP OxD over time of cells transitioned to the dark for 90 minutes (gray box) at time 0 ("dark") and cells kept in light conditions ("light"), n=3. SEM lower than 0.5% are not shown. (*E*) Dead cells fraction 24 h post H_2O_2 treatment, with or without transition to the dark ("dark" and "light" respectively), as measured by positive Sytox staining. Data is shown as mean ± SEM, n=3.

The "oxidized" and "reduced" subpopulations differ in their cell fate.

We further examined the possible link between early chloroplast E_{GSH} oxidation and subsequent cell fate determination. We compared the fraction of the chl-roGFP "oxidized" subpopulation 1-2 hours post H_2O_2 treatments to the fraction of dead cells 24 hours post treatment as measured by Sytox staining (Fig. 3 A). These parameters exhibited a strong correlation (R^2=0.835, slope of the linear fit: 0.945, Fig. 3 A), supporting our hypothesis that detection of early chloroplast oxidation in distinct subpopulations predicts cell fate at much later stages.

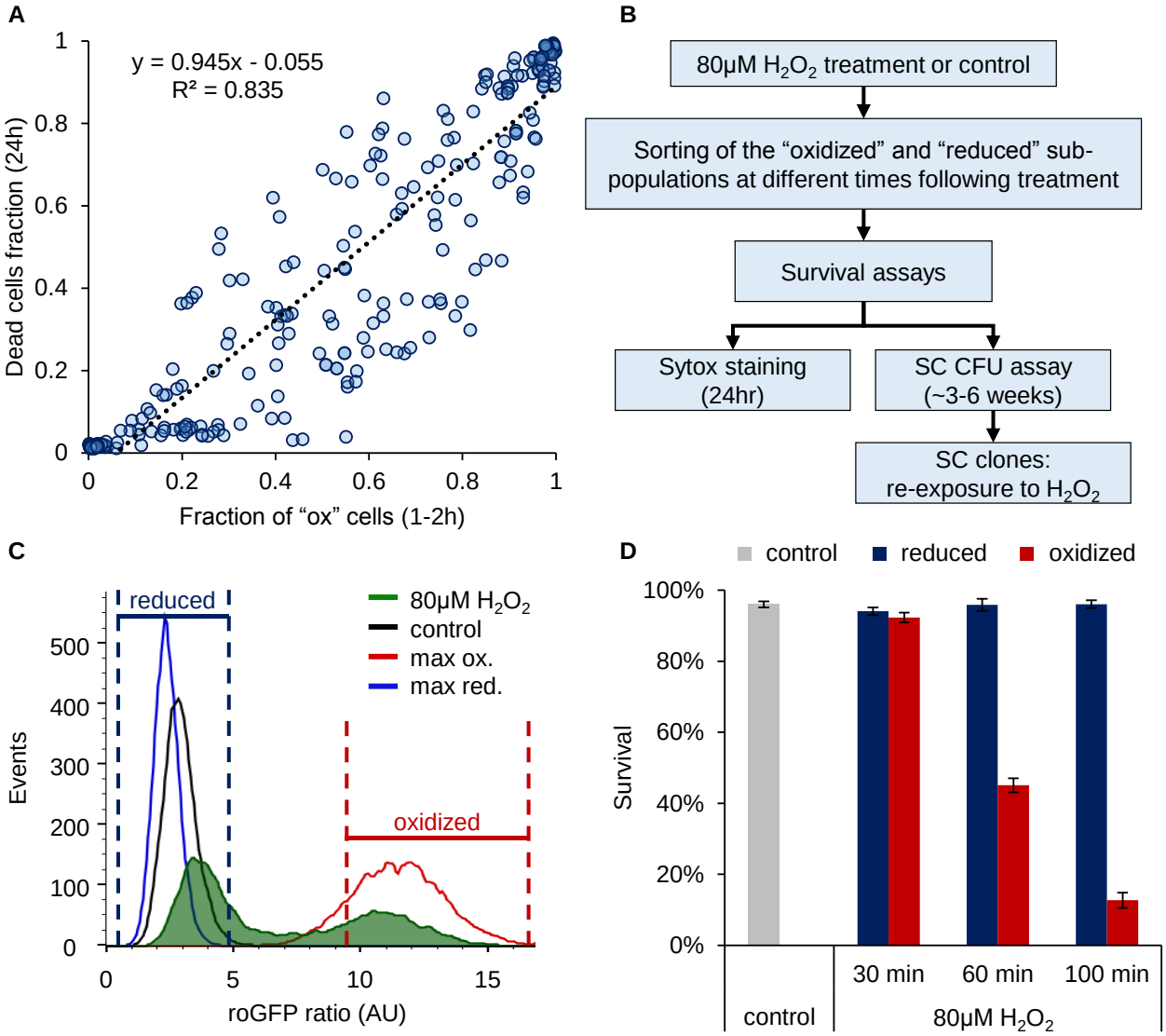

Fig. 3. Early oxidation of chl-roGFP subpopulation leads to subsequent induction of cell death. The link between chl-roGFP early oxidation and subsequent cell death was examined. (*A*) Correlation between the fraction of dead cells 24 h post H_2O_2 treatment, as measured by Sytox positive staining, and the fraction of "oxidized" chl-roGFP subpopulation 1-2 hours post treatment. Data was gathered from 10 independent experiments including 5-200μM H_2O_2 treatments. Each condition was measured with ≥3 repeats, each repeat is represented as one data point, n=263. A linear regression fit is shown as a dashed line. (*B*) Schematic representation of the sorting experiments layout. (*C*) Representative histograms of chl-roGFP oxidation distribution (roGFP ratio, AU) 100 min following 80μM H_2O_2 treatment (green). Maximum oxidation (200μM H_2O_2, red), maximum reduction (2mM DTT, blue), and untreated control (black) are shown for reference. Gates used for sorting the "oxidized" and "reduced" subpopulations based on chl-roGFP oxidation are shown, untreated control cells were sorted based on positive roGFP expression. (*D*) Survival of individual cells that were sorted and regrown, as measured by their ability to form a colony. Data is shown as mean ± SEM, n≥6 biological repeats each of 24-48 sorted single cells per time-point per subpopulation.

To investigate directly the link between early chl-roGFP oxidation and subsequent cell death, we sorted single cells based on chl-roGFP oxidation at different time-points following addition of 80μM H_2O_2 using fluorescence-activated cell sorting (FACS) into fresh media, and measured their survival by their ability to grow and form a colony (Fig. 3 B-D). When sorted 30 minutes post treatment, the "oxidized" subpopulation exhibited a high survival rate of 92.3 ± 1.4%, similar to the "reduced" subpopulation (94.1 ± 1.1%, P=0.32), though slightly but significantly lower than sorted untreated control (96 ± 0.9%, P=0.029, Fig. 3 D). However, at later time-points the survival of the "oxidized" subpopulation gradually diminished. When sorted 60 min

post treatment almost half of the "oxidized" cells were still able to recover (45.1 ± 2%), but only 12.7 ± 2.1% survived following sorting at 100 min (Fig. 3 D). These results suggest that after a distinct exposure time, cell death is induced in an irreversible manner in the "oxidized" subpopulation. In contrast, the "reduced" subpopulation from the same culture and treatment exhibited a high survival rate similar to the control at all time-points examined, demonstrating its resilience to the stress (Fig. 3 D). In agreement with these findings, cell death measurements using Sytox staining of sorted enriched subpopulations also showed higher mortality in the "oxidized" compared to "reduced" and control cells, which remained viable (Fig. S7). Taken together, these results demonstrate that the "oxidized" subpopulation was sensitive to the oxidative stress applied, which led to induction of cell death in those cells, while the "reduced" subpopulation was able to survive. In addition, we revealed a distinct phase of "pre-commitment" to cell death, ranging approximately 30-100 min in most cells, during which the fate of the "oxidized" subpopulation is still reversible upon removal of the stress.

The distinct subpopulations derive from phenotypic variability and not due to variable genetic background.

Next, we investigated whether the differential chloroplast oxidation of the observed subpopulations is due to genetic variability or whether it represents phenotypic plasticity within the population. To this aim, we sorted chl-roGFP individual cells of the "oxidized" and "reduced" subpopulations 30 and 100 minutes post 80µM H_2O_2 treatment as well as untreated control cells, and regrew them to generate clonal populations derived from cells exhibiting specific phenotypes. The clonal progeny cultures were subsequently exposed to 80µM H_2O_2 and their chl-roGFP oxidation was measured. The two distinct subpopulations were detected in all the clones measured, and the fraction of the "oxidized" subpopulation was correlated with cell death (Fig. 4 and Fig. S8). Therefore, the different subpopulations observed did not originate from genetic differences, but rather represent phenotypic variability within clonal populations.

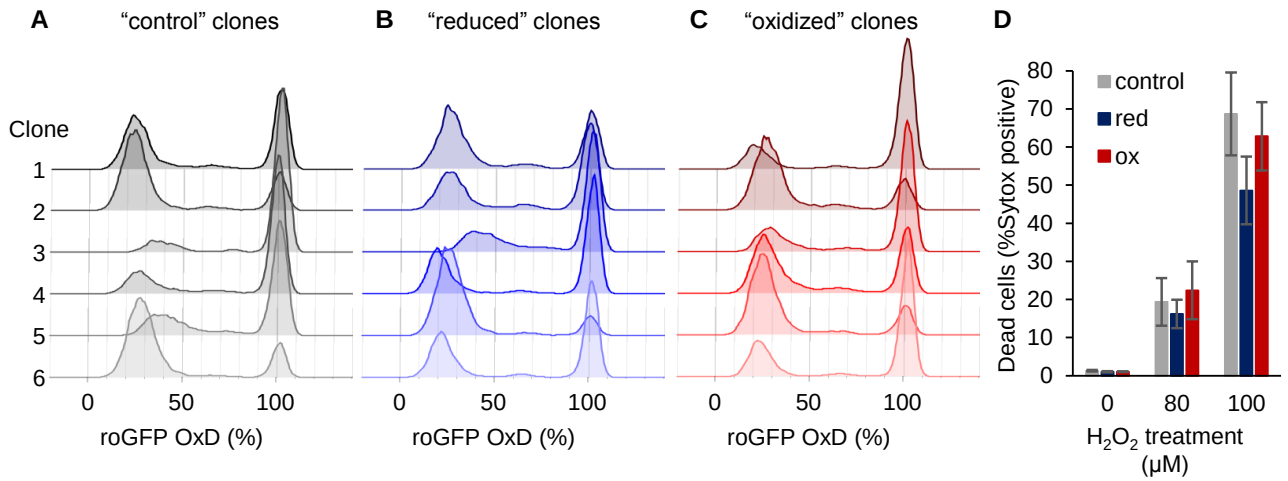

Fig. 4. Sorted clonal populations maintain the bi-stable phenotype in chl-roGFP response to H_2O_2. To investigate whether the differential response of the subpopulations was due to genetic differences, the chl-roGFP response of clonal populations to H_2O_2 was examined. (*A-C*) The distribution of chl-roGFP OxD (%) 40-45 min post 80µM H_2O_2 treatment in clonal populations derived from sorted single cells of different origins, 3 weeks post sorting. The "reduced" (B) and "oxidized" (C) subpopulations were sorted 30 minutes post 80µM H_2O_2 treatment based on chl-roGFP oxidation (Fig. 3C); "control" (A) - untreated sorted cells. Each histogram is of a single clone, ≥9900 cells per histogram, 6 representative clones per group are shown. The same phenomenon was observed in 2 independent experiments in all examined clones

(≥18 clones per group), for visualization data from one experiment is shown. (*D*) The fraction of dead cells 24 h post H_2O_2 treatment of the different clones shown in (A-C) as measured by positive Sytox staining. Data is shown as mean ± SEM, n=6.

Early chloroplast oxidation predicts cell fate at the single-cell level.

In order to track oxidation dynamics and subsequent cell fate of individual cells, we established a microfluidics platform for *in*-vivo long-term epifluorescence imaging adapted for diatom cells, under controlled flow, light and temperature conditions (Fig. 5, Fig. S9 and movies S1, S2). We introduced cells expressing chl-roGFP into a custom-made microfluidics device, and after settlement of the cells we introduced treatments of either 80µM H_2O_2 or fresh media (control) continuously for 2.5-3 hours (see methods). The use of microfluidics enabled also to image the basal state of single cells prior to treatment, as well as the introduction of Sytox green at the end of the experiment to visualize cell viability. We detected the distinct "oxidized" and "reduced" subpopulations following 80µM H_2O_2 treatment, similar to the flow cytometry experiments (Fig. 5 C, F, and movie S1). However, no clear differences were observed in their basal OxD prior to treatment (Fig. S10 and movie S1). The separation between the subpopulations emerged within 20 minutes of exposure to 80µM H_2O_2, and remained stable over the course of the experiment with the "oxidized" subpopulation maintaining a high OxD above 80% (Fig. 5 F, Fig. S10 B and movie S1). The "reduced" subpopulation exhibited an immediate response to the treatment, from 25-45% OxD at basal state to 30-65% OxD during the first 20 minutes post H_2O_2 treatment (Fig. 5 F, Fig. S10 B, and movie S1), comparable with flow cytometry measurements. Following this initial oxidation, the "reduced" cells recovered gradually over the next hours, reducing to 5-25% oxidation 8 hours post treatment, below the initial basal state (Fig. 5 F, movie S1). A gradual slow reduction was also observed in the control cells over the course of the experiment (Fig. 5 E, movie S2), and may represent acclimation to the experimental setup or a diurnal redox alteration. Control cells did not oxidize in response to addition of fresh media (Fig. 5 E and Fig. S10 A), excluding the possibility that the oxidation observed in 80µM H_2O_2 treated cells was due to shear stress during treatment.

We detected a clear correlation between initial oxidation in the chloroplast in response to oxidative stress and subsequent cell fate (Fig. 5 A-G). Cells that exhibited within 42 minutes high chl-roGFP oxidation also underwent cell death at a much later stage, while cells that maintained lower OxD were able to recover and remained viable (Fig. 5 G). The Sytox positive cells showed nuclear staining as expected and lower chlorophyll auto-fluorescence intensity (Fig. 5 D). To discriminate between the "oxidized" and "reduced" subpopulations we used a threshold of 70% roGFP OxD based on clear visible separation (dashed line, Fig. 5 E-G). Using this threshold, the OxD of chl-roGFP at 42 minutes post H_2O_2 treatment predicted subsequent death of individual cells as measured ~23 hours post treatment with high accuracy of 98.8% (1.7% false positive, 0.8% false negative; Fig. 5 G). These results demonstrate that the early response of chloroplast E_{GSH} can be used to make high precision cell fate predictions at the single-cell level.

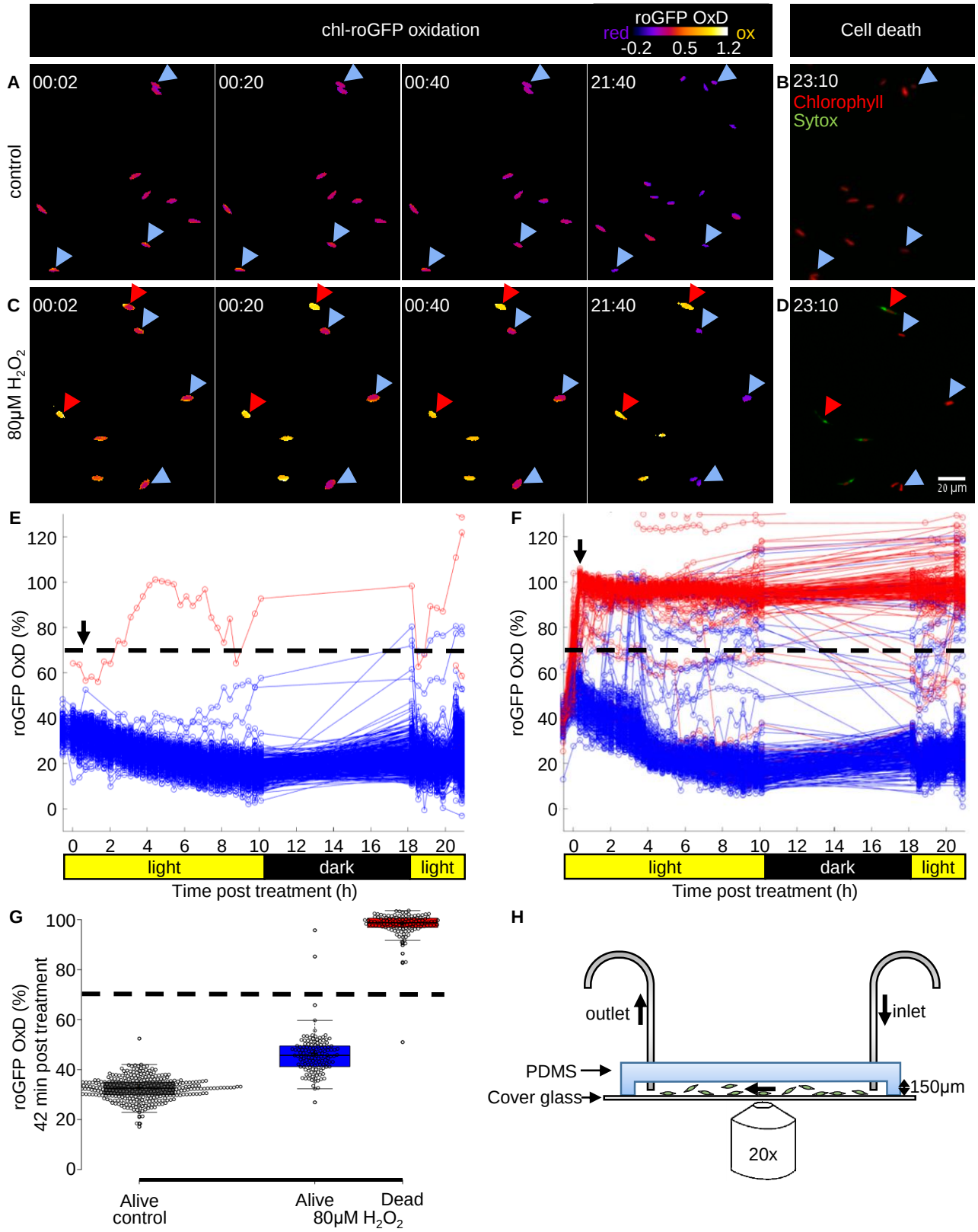

Fig. 5. Tracking redox dynamics of individual cells using *in vivo* imaging in a microfluidics setup. Oxidation of chl-roGFP cells was imaged over time using a customized microfluidic setup and epifluorescence microscopy. Cells were imaged following treatment with either fresh media (control; A, B, E) or 80µM H_2O_2 (C, D, F). To quantify cell death, cells were stained with Sytox ~23 h post treatment. (*A, C*) Representative frames depicted in pseudo-color of calculated roGFP OxD at different times post treatment. Two subpopulations of "oxidized" (red arrows) and "reduced" (blue arrows) cells were detected in treated cells. Time post treatment is shown as hh:mm. (*B, D*) Overlay of Sytox staining (green, dead cells) and chlorophyll auto-fluorescence (red) at 23:10 hours post treatment. (*E, F*) Quantification of chl-roGFP OxD per cell over

time post treatment. Color is based on subsequent cell fate as measured by Sytox staining ~23 h post treatment: blue – alive; red – dead. Horizontal dashed line represents the threshold used for discrimination between the "oxidized" and "reduced" subpopulations and for cell fate predictions. N≥250 tracks from ≥3 different fields. The same phenomenon was observed in at least two independent experiments, data of one experiment is shown. (*G*) Box-plot of chl-roGFP OxD 42 min post treatment (arrow in E, F) of cells that were grouped based on their cell fate. Grey – control alive; blue – 80µM H_2O_2 alive; red – 80µM H_2O_2 dead. Circles - single cells; cross – mean; colored box – 1st to 3rd quartiles; horizontal line within the box – median. N≥250 cells per treatment from ≥3 different fields. (*H*) Side view of the microfluidics chip design.

Discussion

Our current understanding of the mechanisms that mediate acclimation to environmental stressors in marine microorganisms, including diatoms, is derived primarily from observations at the population level, neglecting any heterogeneity at the single-cell level. Averaging the phenotypes of a whole population could mask the co-existence of distinct subpopulations that induce diverse cellular strategies to improve the survival of this globally important phytoplankton group. In this study, we established a novel system for studying phenotypic variability in the marine diatom *P. tricornutum* using flow cytometry and microfluidics live-imaging. Using organelle-specific measurements of E_{GSH} dynamics we assessed the *in vivo* metabolic state of individual diatom cells, and were able to detect a differential response to oxidative stress within the population. We identified two distinct subpopulations that emerged early following exposure to oxidative stress, differing in their chloroplast E_{GSH} and eventual cell fate, demonstrating the importance of phenotypic variability in cell fate regulation in diatoms.

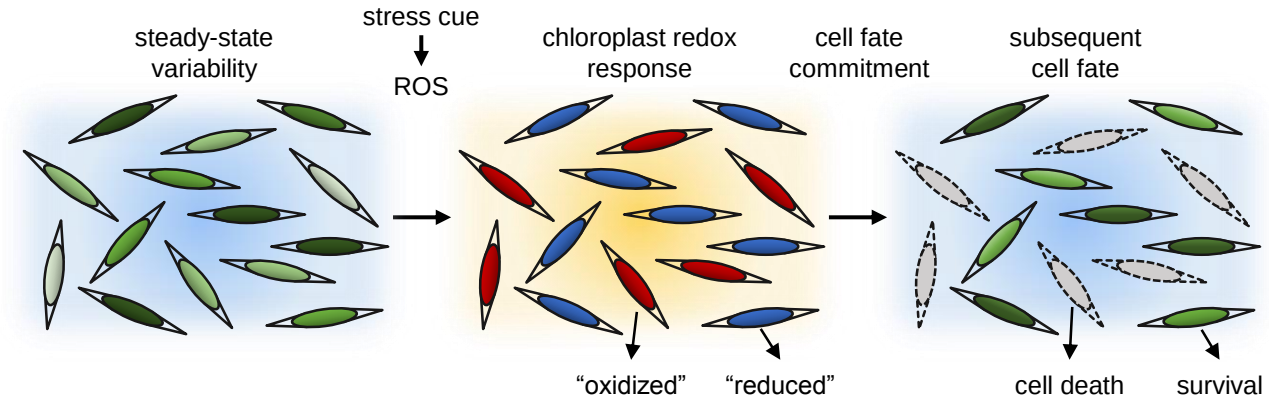

Fig. 6. Proposed redox regulation of cell fate determination in marine diatoms. Phenotypic variability within diatom populations can affect cell fate determination in response to a stress event. We propose that the cell redox state determines the probability of a cell to survive a stress event, and could be affected by various factors such as local ROS levels, antioxidant capacity, metabolic activity, growth phase, cell cycle position, microenvironment etc. If a cell crosses a suggested "death threshold", it is likely to commit to cell death. At steady-state conditions, there is a continuous distribution of metabolic states in the population and most cells are below this threshold. Following a stress event, ROS may accumulate at sub-cellular compartments in the cell, including the chloroplast, and the population distribution will be shifted towards a more oxidized state. The magnitude of the shift depends on the stress applied and the prior metabolic state of the cells, affecting the fraction of cells that will cross the threshold. Depending on these factors, due to the shift some cells will cross the threshold and will commit to cell death, as was observed in the "oxidized" subpopulation. Chloroplast E_{GSH} oxidation is an early stage in this stress response and precedes the commitment to cell fate. Cells that do not cross the threshold, as the "reduced" subpopulation, are able to recover from the stress and survive.

We propose that chloroplast E_{GSH} in diatoms is involved in sensing specific stress cues that induce oxidative stress, and in cell fate regulation (Fig. 6). Depending on the specific stress, ROS can accumulate at various sub-cellular compartments (16, 17), resulting in a shift of the population towards a more oxidized state. Cells that

accumulate ROS above a certain threshold are likely to induce cell death, as observed in the "oxidized" subpopulation (Figs. 5 and 6). Cells that do not cross this threshold are able to recover and acclimate, as detected in the "reduced" subpopulation (Figs. 5 and 6). Using a microfluidics setup that allowed cell tracking during exposure to H_2O_2, we revealed such a "life-death threshold" based on early chl-roGFP oxidation (Fig. 5 G). This early response provided accurate cell fate predictions at the single-cell level. We propose that the balance between the basal metabolic state, the antioxidant capacity, and the magnitude of the applied stress leads to a differential response within the population. This could also explain the increase in the proportion of the "oxidized" subpopulation in a H_2O_2 dose-dependent manner (Fig. 1 M) and may account for the increased sensitivity of the entire population in the absence of light (Fig. 2). Moreover, the later further supports an involvement of the chloroplast in cell fate determination, and suggests that fluctuating light conditions experienced by diatoms in natural environments may greatly affect their susceptibility to additional stressors.

Redox fluctuations in the chloroplast can serve as a rapid mechanism to perceive specific environmental cues, by regulating key metabolic pathways on the post-translational level prior to gene expression. It is notable that chloroplast E_{GSH} oxidation preceded the "point of no return", after which cell death is irreversibly activated (Fig. 3 D). This "pre-commitment" phase provides an opportunity for cells to recover if conditions change during a narrow time frame, which ranges in most of the population between ~30-100 min following the stress event, before the cell has accumulated damage beyond repair (Fig. 3 D). A similar "pre-commitment" phase was shown when diatom cells were rescued from infochemicals or H_2O_2 treatments by exogenous application of the antioxidant GSH only within a similar time frame (16, 18). Furthermore, analysis of the redox-sensitive proteome in *P. tricornutum* revealed over-representation of chloroplast-targeted proteins, that were also oxidized to a greater degree under H_2O_2 treatment as compared to other subcellular compartments (17). These findings underscore the prevalent role of redox regulation in chloroplast metabolic reactions, and may be involved in cell fate determination.

The role of the chloroplast in mediating PCD remains elusive, although mitochondria-generated ROS are known to play a key role in PCD in plants and animals (34, 35). This gap of knowledge is even greater in unicellular marine algae for which the molecular basis for the PCD machinery is largely unknown (8). The chloroplast is a major source for generation of both ROS and reductive power in the form of reduced ferredoxin or NADPH (23). Chloroplast generated ROS were demonstrated to be involved in plants in retrograde signaling from the chloroplast and in hypersensitive response cell death (23, 31, 34, 36). A recent model suggested possible mitochondria-chloroplast cooperative interactions in the execution of ROS-mediated PCD (34). In diatoms, mitochondrial ROS were linked to cell death in response to diatom-derived infochemicals (16), and chloroplast E_{GSH} was shown to mediate changes in oxidative stress sensitivity upon light-dark transitions (18). Taken together with the results presented here, these findings suggest that redox dynamics of both the mitochondria and the chloroplast are involved in cell fate regulation in diatoms.

As universal signaling molecules, ROS have been suggested to play a conserved role in stress sensing and cell fate regulation (22, 34, 37). Interestingly, a similar phenomenon of phenotypic heterogeneity in redox state that was linked to subsequent cell fate was also documented in diverse biological systems. In a mouse model for Alzheimer's disease, E_{GSH} oxidation in a small subpopulation of neurons preceded apoptotic PCD in those cells (38). Mammalian cell lines treated with H_2O_2 revealed two distinct subpopulations that activated genes mediating either pro-survival (through ERK) or pro-apoptotic (through p53) pathways, and the proportions

between these subpopulations were H_2O_2-dose dependent (39). In yeast, subpopulations with different growth arrest phenotypes were detected in response to H_2O_2, and their proportions were also H_2O_2 dose-dependent (40). These findings suggest a functionally conserved role for redox heterogeneity in cell fate determination across kingdoms, and could represent a more general phenomenon.

The mechanism driving the variability observed in our system is yet to be explored, but the results presented here provide insights into factors that can affect it. Since clonal populations originated from single-cell isolation maintained the bi-stable chloroplast response, the source of variability was not genetic differences between the subpopulations (Fig. 4). Inter-individual phenotypic variability is known to exist also in genetically homogenous clonal populations, and can derive from various sources such as cell life history, cell cycle phase, cell age, unequal partitioning of molecules during cell division, metabolic activity, heterogeneous microenvironment and biological noise (41–51). The combination of these factors results in a distribution of cells with different metabolic states within the population (49, 50). The metabolic state of the cell can affect its antioxidant capacity, therefore resulting in variability in sensitivity to oxidative stress as observed in our system. The antioxidant capacity of a cell to detoxify ROS depends on photosynthesis-generated NADPH, which is also used for GSH recycling. Importantly, the chl-roGFP bi-stable pattern was abolished when the cells were under darkness, as the entire population became more sensitive to oxidative stress (Fig. 2). The transition to the dark may have compromised the biosynthesis and recycling of GSH therefore enhancing sensitivity to oxidative stress, as was recently demonstrated in another marine diatom (18). Taken together, heterogeneity in sensitivity to oxidative stress within the population can result from variability in photosynthesis-derived redox equivalents that regulate the antioxidant capacity of the chloroplast.

Phenotypic variability can provide an important strategy to cope with fluctuating environments in microbial populations (44). Co-existence of subpopulations with different susceptibilities to certain stressors can be viewed as a “bet-hedging” strategy of the population, enabling at least a portion of the population to survive unpredicted stress events and subsequently leads to a growth benefit at the population level (44, 46, 52, 53). Furthermore, such variability enables individual cells within isogenic populations to exhibit various cell fates, including PCD, despite possible deleterious effects at the single-cell level. In diatoms, phenotypic variability in cell size, shape and susceptibility to stress conditions were suggested (1, 16, 18, 54). However, until now the experimental setups were not designed to study individuality in stress response. Redox-based phenotypic variability can provide a rapid and adjustable strategy to cope with unpredicted stress conditions as compared to relying only on genetic diversity. There may be a tradeoff between resilience to oxidative stress and the ability to sense with high precision environmental cues and metabolic perturbations (37). Since mild redox perturbations can be used for sensing and acclimation, high ROS buffering capacity may mask some of these signals. In that case, such heterogeneity in oxidative stress sensitivity may provide a benefit under fluctuating environments.

The novel approaches developed here can provide new insights into individuality in marine microbes, and will enable studying dynamic processes at the single-cell level in diatoms and other ecologically relevant microorganisms. Future studies are required to investigate the possible tradeoff between maintaining high antioxidant capacity and the ability to sense environmental cues at high precision. The ecological importance of variability in redox state in the chloroplast and the mechanisms that underlie differential sensitivity to oxidative stress are yet to be explored.

Methods

roGFP measurements: roGFP oxidation was measured using the ratio between two fluorescence channels, i405 and i488, by fluorescence microscopy (see SI methods) and by flow cytometry using BD LSRII analyzer, BD FACS AriaII and BD FACS AriaIII. The roGFP ratio (i405/i488) increases upon oxidation of the probe (55). The oxidation degree of roGFP (OxD) was calculated according to Schwarzländer *et al.* (55):

$$OxD_{roGFP} = \frac{R - R_{red}}{\frac{i488_{ox}}{i488_{red}}(R_{ox} - R) + (R - R_{red})}$$

Where R is the roGFP ratio of i405/i488, R_{red} is the ratio of fully reduced form (15-50 minutes post treatment with 1-2mM DTT), R_{ox} is the ratio of the fully oxidized form (7-30 minutes post treatment with 200µM H_2O_2), and $i488_{ox}$ and $i488_{red}$ are the i488 of the maximum oxidized and maximum reduced forms respectively. In flow cytometry measurements, i405 was measured using ex 407nm, em 530/30nm or 525/25nm, and i488 was measured using ex 488nm, em 530/30nm. Relative expression level of roGFP was measured by multiplication of i405 and i488. The dynamic range of roGFP was calculated by ratio of R_{ox}/R_{red} (table S1). Flow cytometry measurements were done under ambient light and temperature conditions, except for dark treatment during which samples were covered with aluminum foil. For sorting purposes, roGFP ratio was used, as exact OxD cannot be calculated prior to sorting. Both parameters give similar partition between the subpopulations (data not shown).

Microfluidics experiments: Cells were introduced into a pre-washed home-made microfluidics chip. Following settlement on the glass bottom and at least 1 hour after cells were introduced to the system, cells were imaged for roGFP measurements, chlorophyll auto-fluorescence and bright field (BF). Cells were imaged every 20 min to avoid photo-toxicity, and were illuminated between imaging using BF light. After imaging the basal state of the cells, treatments of either 80µM H_2O_2 in fresh media or fresh media control were introduced to the system continuously for ~2.5-3 hours, after which they were gradually washed away by fresh media. To quantify cell death, Sytox green was introduced into the system at 21.5-23 hours post treatment (see SI appendix). Only a small fraction of cells within the control treatment were Sytox positive (0.0054%), indicating that cells remained viable in this experimental setup. Furthermore, cells of the "reduced" subpopulation and of control treatment were able to proliferate, further demonstrating their viability under these conditions (movies S1, S2). Flow rate was kept at 1 µl/min for the duration of the experiment, except during treatment introduction (10 µl/min for the initial 10 minutes for rapid replacement of media), cell introduction (100 µl/min) and cell settlement (up to 20µl/min with occasional stops). Experimental setup is further described in SI appendix and Fig. S9. Data was analyzed using a tailored MATLAB script (Fig. S11, SI appendix).

Additional methods are described in SI appendix.

Acknowledgments

We thank Dr. Vicente I. Fernandez and Prof. Roman Stocker for help with the cell tracking algorithm. We thank Dr. Uri Sheyn for guidance in operating the FACS. We thank Jenny Mizrahi for proofing the manuscript. This research was supported by the Israeli Science Foundation (ISF) (grant #712233) awarded to AV.

References

1. Armbrust EV (2009) The life of diatoms in the world's oceans. *Nature* 459(7244):185–192.

2. Nelson DM, Tréguer P, Brzezinski M a., Leynaert A, Quéguiner B (1995) Production and dissolution of biogenic silica in the ocean: Revised global estimates, comparison with regional data and relationship to biogenic sedimentation. *Global Biogeochem Cycles* 9(3):359.

3. Malviya S, et al. (2016) Insights into global diatom distribution and diversity in the world's ocean. *Proc Natl Acad Sci* 113(11):E1516–E1525.

4. Morel FMM, Price NM (2003) The biogeochemical cycles of trace metals in the oceans. *Science* 300(5621):944–947.

5. Strass VH, Nöthig E-M (1996) Seasonal shifts in ice edge phytoplankton blooms in the Barents Sea related to the water column stability. *Polar Biol* 16(6):409–422.

6. Tréguer P, et al. (2018) Influence of diatom diversity on the ocean biological carbon pump. *Nat Geosci* 11(1):27–37.

7. Bidle KD (2015) The Molecular Ecophysiology of Programmed Cell Death in Marine Phytoplankton. *Ann Rev Mar Sci* 7(1):341–375.

8. Bidle KD (2016) Programmed Cell Death in Unicellular Phytoplankton. *Curr Biol* 26(13):R594–R607.

9. Ianora A, et al. (2006) New trends in marine chemical ecology. *Estuaries and Coasts* 29(4):531–551.

10. Thamatrakoln K, et al. (2013) Death-specific protein in a marine diatom regulates photosynthetic responses to iron and light availability. *Proc Natl Acad Sci* 110(50):20123–20128.

11. Thamatrakoln K, Korenovska O, Niheu a. K, Bidle KD (2012) Whole-genome expression analysis reveals a role for death-related genes in stress acclimation of the diatom *Thalassiosira pseudonana*. *Environ Microbiol* 14(1):67–81.

12. Kimura K, Tomaru Y (2015) Discovery of Two Novel Viruses Expands the Diversity of Single-Stranded DNA and Single-Stranded RNA Viruses Infecting a Cosmopolitan Marine Diatom. *Appl Environ Microbiol* 81(3):1120–1131.

13. van Tol HM, Amin SA, Armbrust EV (2017) Ubiquitous marine bacterium inhibits diatom cell division. *ISME J* 11(1):31–42.

14. Vardi A, et al. (2006) A stress surveillance system based on calcium and nitric oxide in marine diatoms. *PLoS Biol* 4(3):0411–0419.

15. Vardi A, et al. (2007) Synchronization of cell death in a dinoflagellate population is mediated by an excreted thiol protease. *Environ Microbiol* 9(2):360–369.

16. Graff van Creveld S, Rosenwasser S, Schatz D, Koren I, Vardi A (2015) Early perturbation in mitochondria redox homeostasis in response to environmental stress predicts cell fate in diatoms. *ISME J* 9(2):385–395.

17. Rosenwasser S, et al. (2014) Mapping the diatom redox-sensitive proteome provides insight into response to nitrogen stress in the marine environment. *Proc Natl Acad Sci U S A* 111(7):2740–5.

18. Volpert A, Graff van Creveld S, Rosenwasser S, Vardi A (2018) Diurnal fluctuations in chloroplast GSH redox state regulate susceptibility to oxidative stress and cell fate in a bloom-forming diatom. *J Phycol*. doi:10.1111/jpy.12638.

19. Vardi A, et al. (1999) Programmed cell death of the dinoflagellate *Peridinium gatunense* is mediated by CO_2 limitation and oxidative stress. *Curr Biol* 9(18):1061–1064.

20. Mittler R, et al. (2011) ROS signaling: the new wave? *Trends Plant Sci* 16(6):300–309.

21. Suzuki N, Koussevitzky S, Mittler R, Miller G (2012) ROS and redox signalling in the response of plants to abiotic stress. *Plant Cell Environ* 35(2):259–270.

22. D'Autréaux B, Toledano MB (2007) ROS as signalling molecules: mechanisms that generate specificity in ROS homeostasis. *Nat Rev Mol Cell Biol* 8(10):813–824.

23. Dietz K-J, Turkan I, Krieger-Liszkay A (2016) Redox- and Reactive Oxygen Species-Dependent Signaling into and out of the Photosynthesizing Chloroplast. *Plant Physiol* 171(3):1541–1550.

24. Sheyn U, Rosenwasser S, Ben-Dor S, Porat Z, Vardi A (2016) Modulation of host ROS metabolism is essential for viral infection of a bloom-forming coccolithophore in the ocean. *ISME J* 10(7):1–13.

25. Foyer CH, Noctor G (2016) Stress-triggered redox signalling: what's in pROSpect? *Plant Cell Environ* 39(5):951–964.

26. Luo C, et al. (2014) Cellular Responses Associated with ROS Production and Cell Fate Decision in Early Stress Response to Iron Limitation in the Diatom *Thalassiosira pseudonana*. *J Proteome Res* 13(12):5510–5523.

27. Vardi A, et al. (2002) Dinoflagellate-cyanobacterium communication may determine the composition of phytoplankton assemblage in a mesotrophic lake. *Curr Biol* 12(20):1767–1772.

28. Noctor G, Foyer CH (2016) Intracellular redox compartmentation and ROS-related communication in regulation and signaling. *Plant Physiol* 171(July):pp.00346.2016.

29. Owusu-Ansah E, Banerjee U (2009) Reactive oxygen species prime *Drosophila* haematopoietic progenitors for differentiation. *Nature* 461(7263):537–541.

30. Tsukagoshi H, Busch W, Benfey PN (2010) Transcriptional regulation of ROS controls transition from proliferation to differentiation in the root. *Cell* 143(4):606–616.

31. Exposito-Rodriguez M, Laissue PP, Yvon-Durocher G, Smirnoff N, Mullineaux PM (2017) Photosynthesis-dependent H_2O_2 transfer from chloroplasts to nuclei provides a high-light signalling mechanism. *Nat Commun* 8(1):49.

32. Bienert GP, Chaumont F (2014) Aquaporin-facilitated transmembrane diffusion of hydrogen peroxide. *Biochim Biophys Acta* 1840(5):1596–1604.

33. Meyer AJ (2008) The integration of glutathione homeostasis and redox signaling. *J Plant Physiol* 165(13):1390–1403.

34. Van Aken O, Van Breusegem F (2015) Licensed to Kill: Mitochondria, Chloroplasts, and Cell Death. *Trends Plant Sci* 20(11):754–766.

35. Lam E, Kato N, Lawton M (2001) Programmed cell death, mitochondria and the plant hypersensitive response. *Nature* 411(6839):848–853.

36. Liu Y, et al. (2007) Chloroplast-generated reactive oxygen species are involved in hypersensitive response-like cell death mediated by a mitogen-activated protein kinase cascade. *Plant J* 51(6):941–954.

37. Woehle C, Dagan T, Landan G, Vardi A, Rosenwasser S (2017) Expansion of the redox-sensitive proteome coincides with the plastid endosymbiosis. *Nat Plants* 3(6):17066.

38. Xie H, et al. (2013) Rapid cell death is preceded by amyloid plaque-mediated oxidative stress. *Proc Natl Acad Sci U S A* 110(19):7904–9.

39. Nair VD, Yuen T, Olanow CW, Sealfon SC (2004) Early Single Cell Bifurcation of Pro- and Antiapoptotic States during Oxidative Stress. *J Biol Chem* 279(26):27494–27501.

40. Goulev Y, et al. (2017) Nonlinear feedback drives homeostatic plasticity in H_2O_2 stress response. *Elife* 6:1–33.

41. Mathis R, Ackermann M (2016) Response of single bacterial cells to stress gives rise to complex history dependence at the population level. *Proc Natl Acad Sci* 113(15):4224–4229.

42. Stocker R (2012) Marine Microbes See a Sea of Gradients. *Science* 338(6107):628–633.

43. Balaban NQ (2011) Persistence: Mechanisms for triggering and enhancing phenotypic variability. *Curr Opin Genet Dev* 21(6):768–775.

44. Ackermann M (2015) A functional perspective on phenotypic heterogeneity in microorganisms. *Nat Rev Microbiol* 13(8):497–508.

45. Şimşek E, Kim M (2018) The emergence of metabolic heterogeneity and diverse growth responses in isogenic bacterial cells. *ISME J*. doi:10.1038/s41396-017-0036-2.

46. Levy SF, Ziv N, Siegal ML (2012) Bet Hedging in Yeast by Heterogeneous, Age-Correlated Expression of a Stress Protectant. *PLoS Biol* 10(5):e1001325.

47. Graff van Creveld S, Rosenwasser S, Levin Y, Vardi A (2016) Chronic Iron Limitation Confers Transient Resistance to Oxidative Stress in Marine Diatoms. *Plant Physiol* 172(2):968–979.

48. Murik O, Elboher A, Kaplan A (2014) Dehydroascorbate: a possible surveillance molecule of oxidative stress and programmed cell death in the green alga *Chlamydomonas reinhardtii*. *New Phytol* 202(2):471–484.

49. Takhaveev V, Heinemann M (2018) Metabolic heterogeneity in clonal microbial populations. *Curr Opin Microbiol* 45:30–38.

50. Campbell K, Herrera-Dominguez L, Correia-Melo C, Zelezniak A, Ralser M (2018) Biochemical principles enabling metabolic cooperativity and phenotypic heterogeneity at the single cell level. *Curr Opin Syst Biol* 8(December 2017):97–108.

51. Raj A, van Oudenaarden A (2008) Nature, Nurture, or Chance: Stochastic Gene Expression and Its Consequences. *Cell* 135(2):216–226.

52. Schreiber F, et al. (2016) Phenotypic heterogeneity driven by nutrient limitation promotes growth in fluctuating environments. *Nat Microbiol* 1(6):16055.

53. Sengupta A, Carrara F, Stocker R (2017) Phytoplankton can actively diversify their migration strategy in response to turbulent cues. *Nature* 543(7646):555–558.

54. De Martino A, et al. (2011) Physiological and Molecular Evidence that Environmental Changes Elicit Morphological Interconversion in the Model Diatom *Phaeodactylum tricornutum*. *Protist* 162(3):462–481.

55. Schwarzländer M, et al. (2008) Confocal imaging of glutathione redox potential in living plant cells. *J Microsc* 231(2):299–316.